



# UNIVERSITÀ DEGLI STUDI DI TORINO

***This is an author version of the contribution published on:***

*Questa è la versione dell'autore dell'opera:*

*International Journal of Pharmaceutics*

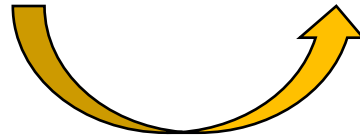
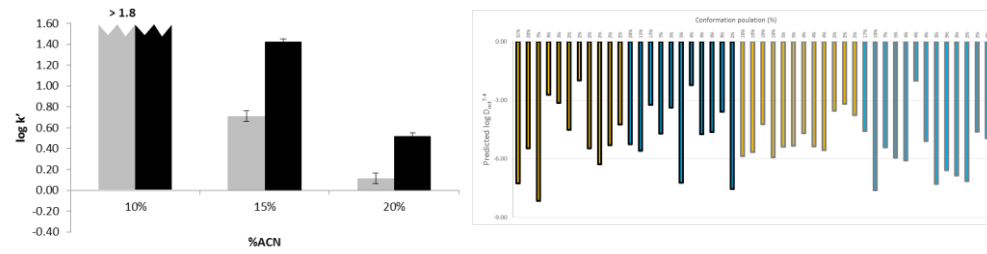
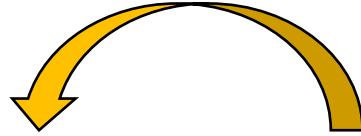
*Volume 495, Issue 1, 2015, Pages 179–185*

*DOI: 10.1016/j.ijpharm.2015.08.075*

***The definitive version is available at:***

*La versione definitiva è disponibile alla URL:*

*<http://www.sciencedirect.com/science/article/pii/S0378517315301708>*



1 Lipophilicity of amyloid  $\beta$ -peptide 12-28  
2 and 25-35 to unravel their skills to  
3 promote hydrophobic and electrostatic  
4 interactions

---

5 G. Ermondi<sup>1</sup>, F. Catalano<sup>2</sup>, M. Vallaro<sup>1</sup>, I. Ermondi<sup>1</sup>, M.P. Camacho Leal<sup>1</sup>, L. Rinaldi<sup>1</sup>, S. Visentin<sup>1</sup>  
6 and G. Caron<sup>1\*</sup>

7 <sup>1</sup> *Molecular Biotechnology and Health Sciences Dept., Università degli Studi di Torino, via*  
8 *Quarello 15, 10135 Torino, Italy.*

9 <sup>2</sup> *Chemistry Dept., Università degli Studi di Torino, Via Giuria 5, 10125, Torino, Italy.*

10

11 E-mail: giulia.caron@unito.it, telephone: +39 011 6708337, fax: +39 011 2357282

12

13 **Keywords**

14 Amyloid peptide, circular dichroism, lipophilicity, molecular dynamics.

15

## 1 **Abstract**

2 The growing interest for peptide therapeutics calls for new strategies to determine the physico-  
3 chemical properties responsible for the interactions of peptides with the environment. This study  
4 reports about the lipophilicity of two fragments of the amyloid  $\beta$ -peptide,  $A\beta_{25-35}$  and  $A\beta_{12-28}$ .

5 Firstly, computational studies showed the limits of  $\log D_{\text{oct}}^{7.4}$  in describing the lipophilicity of  
6 medium-sized peptides.

7 Chromatographic lipophilicity indexes (expressed as  $\log k'$ , the logarithm of the retention factor)  
8 were then measured in three different systems to highlight the different skills of  $A\beta_{25-35}$  and  $A\beta_{12-28}$  in  
9 giving interactions with polar and apolar environments. CD studies were also performed to validate  
10 chromatographic experimental conditions.

11 Results show that  $A\beta_{12-28}$  has a larger skill in promoting hydrophobic and electrostatic interactions  
12 than  $A\beta_{25-35}$ . This finding proposes a strategy to determine the lipophilicity of peptides for drug  
13 discovery purposes but also gives insights in unraveling the debate about the aminoacidic region of  
14  $A\beta$  responsible for its neurotoxicity.

15

## 16 **1. Introduction**

17 In recent years, peptide-based drug discovery has gained a lot of relevance because of good safety,  
18 tolerability and efficacy of peptides. Consequently, there is an important focus on new approaches  
19 to improve the use of peptides in pharmaceutical research (Otvos and Wade, 2014) (Fosgerau and  
20 Hoffmann, 2015).

21 Peptides behavior depends on their skill to interact with the environment (e.g. membranes and  
22 receptors) and on their aggregation properties. For instance, the amyloid  $\beta$ -peptide ( $A\beta$ , a peptide  
23 composed of 39–42 amino acids), is the most abundant component of  $\beta$ -amyloid plaques related to  
24 Alzheimer's disease (AD) (Hardy, 2009). Plaques formation is probably due to the skills of  $A\beta$  to  
25 form aggregates through the interaction with biomembranes (Wood et al., 2003)(Meier and Seelig,  
26 2008)(Dies et al., 2014).

27 Lipophilicity studies provided a lot of information in the understanding of the interaction mechanisms  
28 between classical drugs (i.e. small organic compounds) and the environment (Testa et al., 1996) but  
29 poor information is reported in the literature about peptides.

30 We recently undertook a study to predict lipophilicity of small peptides (maximum length = 6  
31 aminoacids) (Visconti et al., 2015). For these molecules, we found that they could be considered  
32 standard organic structures. However, the most relevant peptides in drug discovery are larger than six  
33 aminoacids and conformational effects are expected to strongly influence their behavior in the human  
34 body.

1 In this study, we characterize the lipophilicity of two flexible peptides of 11 and 17 aminoacids,  
2 respectively. In particular, we unravel the skills of two A $\beta$  fragments, A $\beta$ <sub>25-35</sub> and A $\beta$ <sub>12-28</sub> in  
3 undertaking hydrophobic and polar interaction (the two main components of lipophilicity (El Tayar  
4 et al., 1992)) with polar and apolar environments. It should be recalled that shorter sequences of  
5 A $\beta$  are often used as models of the full-length amyloid peptide, since they are easier to handle.  
6 Computational studies were performed to highlight the limits of log D<sup>7.4</sup><sub>oct</sub> for characterizing the  
7 lipophilicity of the two medium-sized peptides.  
8 Then we measured three chromatographic indexes (expressed as log k') using one reversed-phase  
9 (RP) and two Hydrophilic Interaction Chromatography (HILIC) (Buszewski and Noga, 2012)  
10 systems. The idea is to use two distinguished sets of chromatographic systems to catch the different  
11 skills of the two peptides to engage hydrophobic (RP) and electrostatic interactions (HILIC) with  
12 different environments. The determination of lipophilicity indexes by chromatography is supported  
13 by a number of advantages (e.g. small amounts of material are required, impurities can be separated  
14 during the measurements, there is no need for concentration determination, the process is fast and  
15 can be easily automated) (Poole and Poole, 2003).  
16 CD studies were undertaken to validate some experimental settings used in the chromatographic  
17 determinations.

18

## 19 **2. Material and methods**

20

### 21 **2.1 Materials**

22 A $\beta$ <sub>12-28</sub> and A $\beta$ <sub>25-35</sub> were purchased from Polypeptide Laboratories France (Strasbourg, France,  
23 [www.polypeptide.com](http://www.polypeptide.com)).

24 1,1,1,3,3,3-Hexafluoro-2-propanol (HFIP), acetonitrile (ACN), dimethylsulfoxide (DMSO) and  
25 ammonium acetate were purchased from Alfa Aesar GmbH&Co (Karlsruhe, Germany,  
26 [www.alfa.com](http://www.alfa.com)).

27 Deionized water was used throughout.

28

### 29 **2.2 Circular Dichroism**

30 Solutions of A $\beta$ <sub>12-28</sub> and A $\beta$ <sub>25-35</sub> in the concentration range 30 - 400 $\mu$ M, both in pure HFIP and 10  
31 mM PBS buffer at pH 7.4 + 10% HFIP, were scanned in the far-UV spectral range (four  
32 accumulations) over the wavelength region 180 - 260 nm with a scanning speed of 50 nm/min using  
33 a Jasco J-815 spectropolarimeter equipped with a Xe arc lamp. Spectra were recorded in a quartz

1 circular cuvette (optical path length 0.1 cm). Buffers baselines were subtracted for each  
2 measurement.

3 Secondary structure was estimated from the mean residue ellipticity  $[\theta]$  with the CDNN CD spectra  
4 deconvolution software (Version 2.1, Copyright (C) 1997 Gerald Böhm).

5

## 6 2.3 Chromatography

7 The mobile phase consisted of 20 mM ammonium acetate buffer at pH 7.0 and acetonitrile in  
8 varying proportions. For all mobile phases, the given pH is the pH of the buffer before the addition  
9 of organic modifier.

10 The flow rate was 1 mL/min. The solvent front were used to determine  $t_0$ , i.e., the dead time in RP  
11 systems, toluene was used to determine  $t_0$  under HILIC conditions.

12 HFIP solutions of both peptides were prepared (concentration range of 50-100  $\mu\text{g/mL}$ ) and injected  
13 in the HPLC systems. The choice of HFIP was made on the basis of preliminary tests, which  
14 evidenced the modest solubility of the two peptides in phosphate buffered saline (PBS) and DMSO.  
15 Conversely, they were largely soluble in HFIP.

16 The retention time ( $t_R$ ) were measured on three columns: 1) PLRP-S polymeric reversed phase  
17 column (Agilent, 5cmx4.6mm, 5 $\mu\text{m}$  packing, 100 $\text{\AA}$  pore size); 2) ZIC-HILIC column  
18 (sulfoalkylbetaine zwitterionic phase on a silica gel support, 10 cm  $\times$  4.6 mm, 5 $\mu\text{m}$  packing, 200 $\text{\AA}$   
19 pore size) from SeQuant (Umeå, Sweden) and 3) ZIC-cHILIC column (phosphorylcholine  
20 zwitterionic phase on a silica gel support, 10 cm  $\times$  4.6 mm, 3 $\mu\text{m}$  packing, 100 $\text{\AA}$  pore size) from  
21 SeQuant (Umeå, Sweden). Measures were performed in triplicate.

22 The chromatographic indexes are expressed as  $\log k'$  (Eq. 1)

23

$$24 \log k' = \log ((t_R - t_0)/t_0) \quad \text{Eq. 1}$$

25

26 where  $k'$  is the retention factor,  $t_R$  is the retention time and  $t_0$  is the dead time.

27 A HPLC Varian ProStar instrument equipped with a 410 autosampler, a PDA 335 LC Detector and  
28 Galaxie Chromatography Data System Version 1.9.302.952 was used.

## 29 2.4 Ionization and calculated lipophilicity

30 Ionization constants were calculated with MoKa (Version 2.5.4, <http://www.moldiscovery.com>);  $\log$   
31  $D^{7.4}_{\text{oct}}$  values were calculated with a model recently published by some of us (Visconti et al., 2015).

32

## 1 2.5 Molecular Dynamics simulations

2 All simulations and analysis described below were done using the AMBER14 package that also  
3 includes the trajectory analysis software AmberTools and the module xLEaP used to prepare  
4 starting structures (Case et al., 2012). In particular, MM minimizations and MD simulations were  
5 performed using sander and pmemd modules, respectively.

6 The starting structures of A $\beta$ <sub>12-28</sub> and A $\beta$ <sub>25-35</sub> were obtained from the crystallographic structure of  
7 A $\beta$ <sub>1-42</sub> (PDB id: 1IYT) after deleting unnecessary aminoacids. MD simulations were performed  
8 with constant protonation states for titrable residues. Peptides were modeled in the electrical state  
9 dominating at pH = 7.0. Histidine was considered neutral and the  $\epsilon$ -tautomer was used in the  
10 simulations according to default AMBER choice and to MoKa prediction.

11 Input files were prepared submitting all starting structures to the xLEaP module. The ff99SB force  
12 field was employed.

13 During the chromatographic experiments, peptides experience different environments that depend  
14 on the eluent composition. To obtain reliable simulations we tried to approach the experimental  
15 conditions used to register chromatograms. In particular, we considered two limit conditions. In the  
16 first, epsilon was fixed at 78.5 to mimic an aqueous environment. The second epsilon was set at  
17 37.5 to mimic acetonitrile. Solvation effects for the investigated solvents (water and acetonitrile)  
18 were incorporated using the pairwise Generalized Born model with parameters described by Tsui  
19 and Case (Tsui and Case, 2000). This model uses the default radii set up by xLEaP.

20 Before launching MD simulations, all atoms were optimized without any constrain (500 cycles of  
21 steepest descent followed by 500 cycles of conjugate gradient minimization). After minimization,  
22 all systems were gradually heated from 0 to 325 K with a time step of 0.5 fs over a period of 35 ps.  
23 The temperature plot was used to confirm the attainment of the equilibrium of the heating phase.  
24 Finally, 50 ns MD simulations were performed with a time step of 2 fs. During the MD simulations,  
25 the atom coordinates were saved every 500 steps. All the covalent bonds involving hydrogen atoms  
26 were constrained with the SHAKE algorithm and the Berendsen thermostat was used, both as  
27 implemented in AMBER14. For temperature control a heat bath coupling of 1.0 ps and 0.5 ps were  
28 used during heating and MD simulation, respectively.

29 The MD Movie tool of USCF Chimera (Version 1.10, <http://www.cgl.ucsf.edu/chimera>) was used to  
30 cluster the trajectories based on pairwise best-fit root-mean-square deviations (RMSDs) calculated  
31 on the backbone atoms and to identify a representative frame for each cluster. For any peptide we  
32 considered those clusters that taken together include about 80% of the entire population of  
33 conformers.

1 For validation purposes it should be mentioned that the most stable structure of A $\beta$ <sub>1-42</sub> obtained with  
2 our approach (data not shown) is in agreement with that reported in the literature (Kobayashi and  
3 Takahashi, 2010). This result represents therefore an indirect validation of the applied  
4 computational method.

5 Processing was done on a two 8 cores Xeon E5 at 3.3GHz CPUs and 128GB of RAM.

### 7 **3. Results and discussion**

#### 9 3.1 Ionization

10 The 2D chemical structures of A $\beta$ <sub>12-28</sub> and A $\beta$ <sub>25-35</sub> are shown in Figure 1. A $\beta$ <sub>12-28</sub> has five basic  
11 centers and three acidic centers. All but histidine residues are fully ionized at physiological pH (in  
12 blue basic centers and in red acidic groups, Figure 1). A $\beta$ <sub>25-35</sub> bears two basic (in blue) and one  
13 acidic (in red) groups, completely ionized at pH = 7.0. Summing up, at pH = 7.0 the net charge of  
14 A $\beta$ <sub>12-28</sub> is 0 (three positive and three negative charges), whereas the net charge of A $\beta$ <sub>25-35</sub> is +1 (two  
15 positive and one negative charges).

16  
17 *Please insert Figure 1 here*

#### 19 3.2 Lipophilicity

20 The most commonly used measure of lipophilicity is  $\log D^{7.4}_{\text{oct}}$ . Calculation of  $\log D^{7.4}_{\text{oct}}$  of the  
21 two peptides could be determined using a tool recently reported in the literature by some of us  
22 (Visconti et al., 2015). Since the method uses as an input the 3D structure of the investigated  
23 peptide, MD simulations of the monomeric form of A $\beta$ <sub>12-28</sub> and A $\beta$ <sub>25-35</sub> were performed in two  
24 environments (polar and apolar, see the MD simulations Section for more details) and some  
25 representative conformers were identified through cluster analysis. In particular, 11 conformers  
26 were retained for A $\beta$ <sub>12-28</sub> in both environments whereas 12 and 13 conformers were considered for  
27 A $\beta$ <sub>25-35</sub> in apolar and polar media, respectively.

28 All the representative conformations were submitted to the aforementioned tool (Visconti et al.,  
29 2015) to predict  $\log D^{7.4}_{\text{oct}}$ . Results are summarized in Figure 2.

30  
31 *Please insert Figure 2 here*

32



1 Predicted  $\log D_{\text{oct}}^{7.4}$  in Figure 2 outline that both peptides are very hydrophilic and thus their  $\log$   
2  $D_{\text{oct}}^{7.4}$  may be experimentally inaccessible through standard experimental techniques (e.g. shake-  
3 flask, potentiometry). Please note that when calculated  $\log D_{\text{oct}}^{7.4}$  are considered, caution should be  
4 exercised since the model on which the prediction is based was developed using a dataset of small  
5 peptides (Visconti et al., 2015).

6 Moreover, data in Figure 2 show that  $\log D_{\text{oct}}^{7.4}$  is strongly dependent on conformational changes in  
7 both environments (apolar=yellow; polar=cyan). This represents a major issue in the prediction of  
8  $\log D_{\text{oct}}^{7.4}$  of investigated peptides but it is also expected that this result could be generalized and  
9 extended to most medium-sized peptides.

10 The limits of prediction called for experimental determinations. In particular, we measured the  
11 lipophilicity of A $\beta_{12-28}$  and A $\beta_{25-35}$  using a set of chromatographic lipophilicity indexes.

12 The determination of chromatographic lipophilicity indexes is widely applied to small organic  
13 molecules. The application to peptides is less common and thus some precautions were taken. In  
14 particular, since peptides could form aggregates, HFIP solutions of both samples were injected in  
15 the HPLC systems (see CD measurements).

16 Three chromatographic systems which show a different predominant mechanism of interaction with  
17 the solutes (Ermondi and Caron, 2012) were selected. Their main features are reported in Table 1.

18 The PLRP-S is a reversed phase (RP) system and thus solutes retention is mostly due to  
19 hydrophobic interactions between the solutes and the system (Ermondi and Caron, 2012). On the  
20 contrary, the HILIC systems, which are characterized by zwitterionic stationary phases, are  
21 expected to mainly describe electrostatic, polar and hydrogen bond (HB) interactions (Ermondi and  
22 Caron, 2012). Moreover, to get more specific information in the nature of electrostatic interactions,  
23 we used two HILIC systems which differ in the spatial orientation of the positive and negative  
24 charged groups (Di Palma et al., 2011).

25

26 *Please insert Table 1 here*

27

28 Retention factors were firstly determined using the polymeric PLRP-S column with a mobile phase  
29 containing small quantities of ACN due to the high polarity of the two peptides (Figure 3A). To  
30 obtain the maximum retention under RP conditions, the most non-polar available column should be  
31 used and thus we preferred the PLRP-S to either C8 or C18 columns. Under these conditions the  $\log$   
32  $k'$  value of A $\beta_{12-28}$  is larger than that of A $\beta_{25-35}$  (Figure 3A). This is an expected result since A $\beta_{12-28}$  is  
33 larger than A $\beta_{25-35}$  in any environment (see MD results, Figure S1 in the Supplementary Material)

1 and thus should be retained more by a RP system whose retention is predominantly due to  
2 hydrophobicity (Ermondi and Caron, 2012).

3 In RP systems we expect that  $\log k'$  decreases when the amount of organic solvent in the mobile  
4 phase increases. This was verified as shown in Figure 3A. An additional increase of the amount of  
5 acetonitrile in the mobile phase cannot be checked since under these experimental conditions the  
6 two peptides elute together with the solvent front ( $t_0 = t_R$ ).

7

8 *Please insert Figure 3 here*

9

10 In order to characterize peptides polar properties, peptides retention was also determined using  
11 direct chromatographic systems (i.e. the HILIC and C-HILIC systems, see Table 1). This is a  
12 crucial step which distinguishes strategies for determining lipophilicity of peptides from those  
13 applied to small organic molecules. Peptides in fact are generally more ionized than classical drugs  
14 and thus have more propensity to form electrostatic interaction with the environment. This feature  
15 has to be determined with polar systems.

16 Figure 3B and 3C show that  $A\beta_{12-28}$  is more retained on the HILIC columns than  $A\beta_{25-35}$ . This could  
17 be ascribed to the larger number of ionized centers present on  $A\beta_{12-28}$ , which favor the interaction  
18 with the zwitterionic moiety present on the column surface.

19 The recently developed C-HILIC system differs from the HILIC for the structure and orientation of  
20 the zwitterionic group present on the stationary phase (Table 1). These structural differences should  
21 permit to discriminate positively from negatively charged compounds.  $A\beta_{25-35}$  has an excess of  
22 positive charges and thus we expected that it has a larger affinity for the HILIC system in which the  
23 negative charge is more accessible than the positive one. Unexpectedly, results show that the C-  
24 HILIC system provides similar information than the HILIC system suggesting that the peptides  
25 interaction with HILIC and C-HILIC depends on a complex balance of factors not simply due to the  
26 number and nature of molecular charges but also on conformational effects. Additional studies are  
27 in progress to generalize this finding.

28 Taken together chromatographic data show that  $A\beta_{12-28}$  has a larger skill to interact with both apolar  
29 and polar environments than  $A\beta_{25-35}$ .

30

### 31 3.3 Circular dichroism (CD) studies

32 CD studies were undertaken to unravel a) the influence of HFIP on the solutions injected in the  
33 HPLC systems and b) the propensity of the two peptides to self-aggregation.

1 The effect of HFIP on the secondary structure of peptides and proteins is largely controversial in the  
2 literature. Some reports attribute to HFIP a denaturing effect (Wei and Shea, 2006) whereas others  
3 consider such non-polar organic solvent ( $\epsilon = 16.7$ ) a disaggregating agent or an inductor and  
4 stabilizer of  $\alpha$ -helix structures (Yanagi et al., 2011) (Ryan et al., 2013).

5 Increasing concentrations (30, 125, 250 and 400  $\mu\text{M}$ ) of both peptides were dissolved in pure HFIP  
6 and in PBS at pH 7.4 added with 10% v/v of HFIP (hereafter called  $\text{PBS}_{\text{HFIP}}$ ). Solutions were  
7 analyzed by CD immediately after their preparation (Figure 4 and 5, panel A and B).  $\text{PBS}_{\text{HFIP}}$   
8 solutions were also submitted to CD analysis 24h after preparation (Figure 4 and 5, panel C).

9 The CD profiles of  $\text{A}\beta_{12-28}$  (Figure 4A and B) and  $\text{A}\beta_{25-35}$  (Figure 5A and B) in  $\text{PBS}_{\text{HFIP}}$  are completely  
10 different from those registered in HFIP. In particular, HFIP favors unordered conformations. The  
11 PBS buffer seems to better stabilize ordered conformations of both peptides, favoring an increase of  
12  $\alpha$ -helices and  $\beta$ -sheet structures (more details about interpretation of CD spectra are reported in the  
13 Supplementary Material).

14

15 *Please insert Figure 4 here*

16

17 *Please insert Figure 5 here*

18

19 Self-aggregation phenomena could be present under chromatographic conditions where peptides  
20 concentration was about 400  $\mu\text{M}$ . CD spectra analysis also reveals a substantial difference between  
21 the two analyzed samples after 24 hours (Figures 4 and 5, panel C): while the  $\text{A}\beta_{12-28}$  tends to form  
22 agglomerates marked by the increase in intermolecular  $\beta$ -sheets, the  $\text{A}\beta_{25-35}$  amyloid maintains a  
23 shape of the spectra indicative of a very high percentage of disordered structures. These results  
24 suggests that  $\text{A}\beta_{12-28}$  has a higher propensity to self-assembly than  $\text{A}\beta_{25-35}$ . To avoid self-aggregation,  
25 chromatograms were obtained immediately after samples preparation.

26

## 27 **4. Conclusion**

28 This study provides some general guidelines about the determination of the lipophilicity of  
29 medium-sized peptides. In particular, we evidenced that peptides lipophilicity cannot be properly  
30 determined by traditional descriptors such as  $\log D_{\text{Oct}}^{7.4}$  for two main reasons: a) peptides are too  
31 polar and thus  $\log D_{\text{Oct}}^{7.4}$  is experimentally inaccessible, b) predictions of  $\log D_{\text{Oct}}^{7.4}$  are unreliable  
32 because of the peptides conformational variability. Moreover, lipophilicity varies with the

1 environment and thus the octanol/water system is insufficient to mimic the different biological  
2 conditions.

3 To overcome these limits and to determine the physico-chemical profile of peptides for drug  
4 discovery purposes a set of three chromatographic descriptors have been proposed. In particular, we  
5 characterized the lipophilicity of  $A\beta_{12-28}$  and  $A\beta_{25-35}$  under RP, HILIC and C-HILIC conditions.  
6 Taken together log  $k'$  data showed that  $A\beta_{12-28}$  has a larger skill to interact with hydrophobic and  
7 polar media than  $A\beta_{25-35}$ . Moreover, the two HILIC systems provided similar log  $k'$  values for  $A\beta_{12-28}$   
8 and  $A\beta_{25-35}$ . This was an unexpected result for  $A\beta_{25-35}$  since its net charge is +1 and thus a larger  
9 retention on the HILIC than on the C-HILIC column was expected.

10 Since  $A\beta_{12-28}$  and  $A\beta_{25-35}$  are used as models of the amyloid peptide, these results definitively may  
11 improve the understanding of  $A\beta$  neurotoxicity, which originates from its interaction with lipid  
12 membranes. In general terms, the interaction of compounds with biomembranes is driven by two  
13 main mechanisms. The first is due to hydrophobic interactions with the alkyl chains of  
14 phospholipids, whereas the second is related to electrostatic interactions with their polar heads (van  
15 Balen et al., 2004). Since we proved that  $A\beta_{12-28}$  has more propensity to form both types of  
16 interactions, the region of  $A\beta$  comprised between residues 12 and 28 is expected to be the  
17 responsible for the toxicity of the whole peptides. This contributes to unravel the discussion  
18 reported in the literature about this topic (Liu et al., 2004).

19

## 20 **Acknowledgement**

21 This work has been supported by Ateneo Compagnia di San Paolo-2012-Call 2, LIMPET project.

22

## 1 **References**

- 2 Buszewski, B., Noga, S., 2012. Hydrophilic interaction liquid chromatography (HILIC)--a powerful  
3 separation technique. *Anal. Bioanal. Chem.* 402, 231–47. doi:10.1007/s00216-011-5308-5
- 4 Case DA, Darden TA, Cheatham TE, Simmerling CL, Wang J, Duke RE, Luo R, Walker RC,  
5 Zhang W, Merz KM, Roberts B, Hayik S, Roitberg A, Seabra G, Swails J, Goetz AW,  
6 Kolossváry I, Wong KF, Paesani F, Vanicek J, Wolf RM, Liu J, Wu X, Brozell SR,  
7 Steinbrecher T, Gohlke H, Cai Q, Ye X, Wang J, Hsieh MJ, Cui G, Roe DR, Mathews DH,  
8 Seetin MG, Salomon-Ferrer R, Sagui C, Babin V, Luchko T, Gusarov S, Kovalenko A,  
9 Kollman, PA. AMBER 12. University of California, San Francisco. (2012).
- 10 Di Palma, S., Boersema, P.J., Heck, A.J.R., Mohammed, S., 2011. Zwitterionic hydrophilic  
11 interaction liquid chromatography (ZIC-HILIC and ZIC-cHILIC) provide high resolution  
12 separation and increase sensitivity in proteome analysis. *Anal. Chem.* 83, 3440–3447.  
13 doi:10.1021/ac103312e
- 14 Dies, H., Topozini, L., Rheinstädter, M.C., 2014. The interaction between amyloid- $\beta$  peptides and  
15 anionic lipid membranes containing cholesterol and melatonin. *PLoS One* 9(6), e99124.  
16 doi:10.1371/journal.pone.0099124
- 17 El Tayar, N., Tsai, R.S., Carrupt, P.-A., Testa, B., 1992. Octan-1-ol–water partition coefficients of  
18 zwitterionic  $\alpha$ -amino acids. Determination by centrifugal partition chromatography and  
19 factorization into steric/hydrophobic and polar components. *J. Chem. Soc., Perkin Trans. 2* 79–  
20 84. doi: 10.1039/P29920000079
- 21 Ermondi, G., Caron, G., 2012. Molecular interaction fields based descriptors to interpret and  
22 compare chromatographic indexes. *J. Chromatogr. A* 1252, 84–9.  
23 doi:10.1016/j.chroma.2012.06.069
- 24 Fosgerau, K., Hoffmann, T., 2015. Peptide therapeutics: current status and future directions. *Drug*  
25 *Discov. Today* 20, 122–128. doi:10.1016/j.drudis.2014.10.003
- 26 Hardy, J., 2009. The amyloid hypothesis for Alzheimer's disease: A critical reappraisal. *J.*  
27 *Neurochem.* 110, 1129–1134. doi:10.1111/j.1471-4159.2009.06181.x
- 28 Kelly S.M., Jess T.J., Price N.C.; 2005. *Biochim. Biophys. Acta.* 1751, 119-139.  
29 doi:10.1016/j.bbapap.2005.06.005
- 30 Kobayashi, K., Takahashi, O., 2010. Molecular-Dynamics Simulations for Amyloid  $\beta$  1 – 42  
31 Monomer with d-Aspartic Acid Residues Using Continuous Solvent. *Chem. Biodivers.* 7,  
32 1357–1363. doi: 10.1002/cbdv.200900299
- 33 Liu, R., McAllister, C., Lyubchenko, Y., Sierks, M.R., 2004. Residues 17-20 and 30-35 of Beta-  
34 Amyloid Play Critical Roles in Aggregation. *J. Neurosci. Res.* 75, 162–171.  
35 doi:10.1002/jnr.10859
- 36 Meier, M., Seelig, J., 2008. Length Dependence of the Coil -  $\beta$  -Sheet Transition in a Membrane  
37 Environment. *Biochemistry* 1017–1024. doi: 10.1021/ja077231r

- 1 Otvos, L., Wade, J.D., 2014. Current challenges in peptide-based drug discovery. *Front. Chem.* 2,  
2 8–11. doi:10.3389/fchem.2014.00062
- 3 Poole, S.K., Poole, C.F., 2003. Separation methods for estimating octanol–water partition  
4 coefficients. *J. Chromatogr. B* 797, 3–19. doi:10.1016/j.jchromb.2003.08.032
- 5 Ryan, T.M., Caine, J., Mertens, H.D.T., Kirby, N., Nigro, J., Breheney, K., Waddington, L.J.,  
6 Streltsov, V. a, Curtain, C., Masters, C.L., Roberts, B.R., 2013. Ammonium hydroxide  
7 treatment of A $\beta$  produces an aggregate free solution suitable for biophysical and cell culture  
8 characterization. *PeerJ* 1, e73. doi:10.7717/peerj.73
- 9 Testa, B., Carrupt, P.-A., Gaillard, P., Tsai, R.S., 1996. Intramolecular Interactions Encoded in  
10 Lipophilicity: Their Nature and Significance, in: Pliska, V., Testa, B., van de Waterbeemd, H.  
11 (Eds.), *Lipophilicity in Drug Action and Toxicology*. Wiley-VCH Verlag GmbH & Co. KGaA,  
12 pp 49-71.
- 13 Tsui, V., Case, D. a., 2000. Theory and applications of the Generalized Born solvation model in  
14 macromolecular simulations. *Biopolymers* 56, 275–291. doi:10.1002/1097-  
15 0282(2000)56:4<275::AID-BIP10024>3.0.CO;2-E
- 16 Van Balen, G.P., Martinet, C. a M., Caron, G., Bouchard, G., Reist, M., Carrupt, P.-A., Fruttero, R.,  
17 Gasco, A., Testa, B., 2004. Liposome/water lipophilicity: methods, information content, and  
18 pharmaceutical applications. *Med. Res. Rev.* 24, 299–324. doi:10.1002/med.10063
- 19 Visconti, A., Ermondi, G., Caron, G., Esposito, R., 2015. Prediction and interpretation of the  
20 lipophilicity of small peptides. *J. Comput. Aided. Mol. Des.* 29, 361–370. doi:10.1007/s10822-  
21 015-9829-4
- 22 Wei, G., Shea, J., 2006. Effects of Solvent on the Structure of the Alzheimer Amyloid- b ( 25 – 35 )  
23 Peptide 91, 1638–1647. doi:10.1529/biophysj.105.079186
- 24 Wood, W.G., Eckert, G.P., Igbavboa, U., Müller, W.E., 2003. Amyloid beta-protein interactions  
25 with membranes and cholesterol: Causes or casualties of Alzheimer’s disease. *Biochim.*  
26 *Biophys. Acta - Biomembr.* 1610, 281–290. doi:10.1016/S0005-2736(03)00025-7
- 27 Yanagi, K., Ashizaki, M., Yagi, H., Sakurai, K., Lee, Y., Goto, Y., 2011. Hexafluoroisopropanol  
28 Induces Amyloid Fibrils of Islet Amyloid Polypeptide by Enhancing Both Hydrophobic and  
29 Electrostatic Interactions \* □ 286, 23959–23966. doi:10.1074/jbc.M111.226688

30

## 1 **Figure Captions**

2

3 **Figure 1.** The chemical structures of the two peptides. Acidic centers ionized at pH=7.0 are in red  
4 whereas basic centers ionized at the same pH are in blue. A) A $\beta_{12-28}$  and B) A $\beta_{25-35}$ .

5

6 **Figure 2.** Predicted  $\log D^{7.4}_{\text{oct}}$  of the representative conformers resulting from MD simulations  
7 performed in the two different environments that mimic acetonitrile ( $\epsilon=37.5$  in cyan) and water  
8 ( $\epsilon=78.5$  in yellow) solvent, respectively. A $\beta_{12-28}$  is in black, A $\beta_{25-35}$  is in grey.

9

10 **Figure 3.** Lipophilicity data. A $\beta_{12-28}$  is in black, A $\beta_{25-35}$  is in grey. A) PLRP-S, B) HILIC, C)  
11 HILIC.

12

13 **Figure 4.** CD spectra of A $\beta_{12-28}$  in pure HFIP A), in PBS<sub>HFIP</sub> B) and in PBS<sub>HFIP</sub> 24 h after samples  
14 preparation C) are reported in the top panels at increasing concentration 30, 150, 250 and 400 $\mu$ M  
15 (corresponding to lines a, b, c and d respectively). CD spectra of pure secondary structures as  
16 indicated in literature ( $\alpha$ -helix,  $\beta$ -sheet, turns and random coils corresponding to lines  $\alpha$ ,  $\beta$ , t and rc  
17 respectively) are reported in the bottom panels for the sake of a qualitative comparison (Kelly et al.  
18 2005).

19

20 **Figure 5.** CD spectra of A $\beta_{25-35}$  in pure HFIP A), in PBS<sub>HFIP</sub> B) and in PBS<sub>HFIP</sub> 24 h after samples  
21 preparation C) are reported in the top panels at increasing concentration 30, 150, 250 and 400 $\mu$ M  
22 (corresponding to lines a, b, c and d respectively). CD spectra of pure secondary structures as  
23 indicated in literature ( $\alpha$ -helix,  $\beta$ -sheet, turns and random coils corresponding to lines  $\alpha$ ,  $\beta$ , t and rc  
24 respectively) are reported in the bottom panels for the sake of a qualitative comparison (Kelly et al.  
25 2005).

Table 1. Features of the four chromatographic systems used in the paper

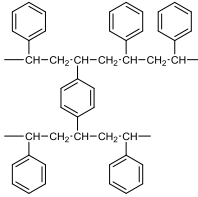
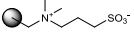
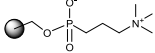
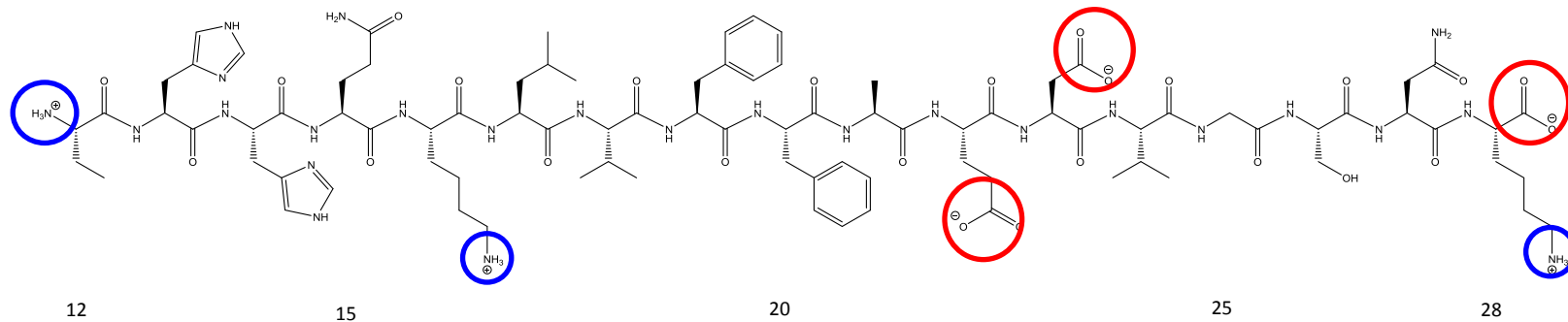
Name	Type	Stationary phase	Interaction
PLRP-S	reversed	 <p> <math>\text{---CH---CH}_2\text{---CH---CH}_2\text{---CH---CH}_2\text{---CH---}</math>  <math>\text{---CH---CH}_2\text{---CH---CH}_2\text{---CH---}</math> </p>	hydrophobic
HILIC	direct	 <p> <math>\text{---N}^+(\text{CH}_3)_2\text{---CH}_2\text{---CH}_2\text{---CH}_2\text{---SO}_3^-</math> </p>	ionic
C-HILIC	direct	 <p> <math>\text{---O---P(=O)(O}^-\text{)---O---CH}_2\text{---CH}_2\text{---CH}_2\text{---N}^+(\text{CH}_3)_2</math> </p>	ionic



Figure 1

Figure 1

A



B

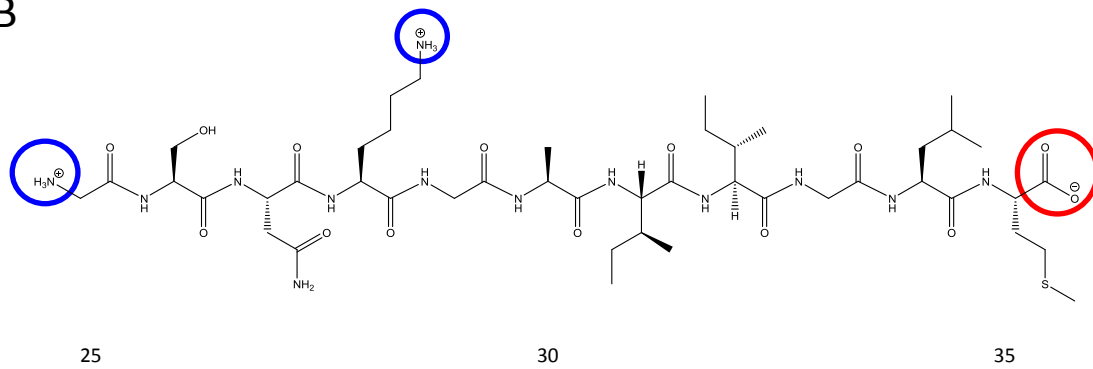


Figure 2

Figure 2

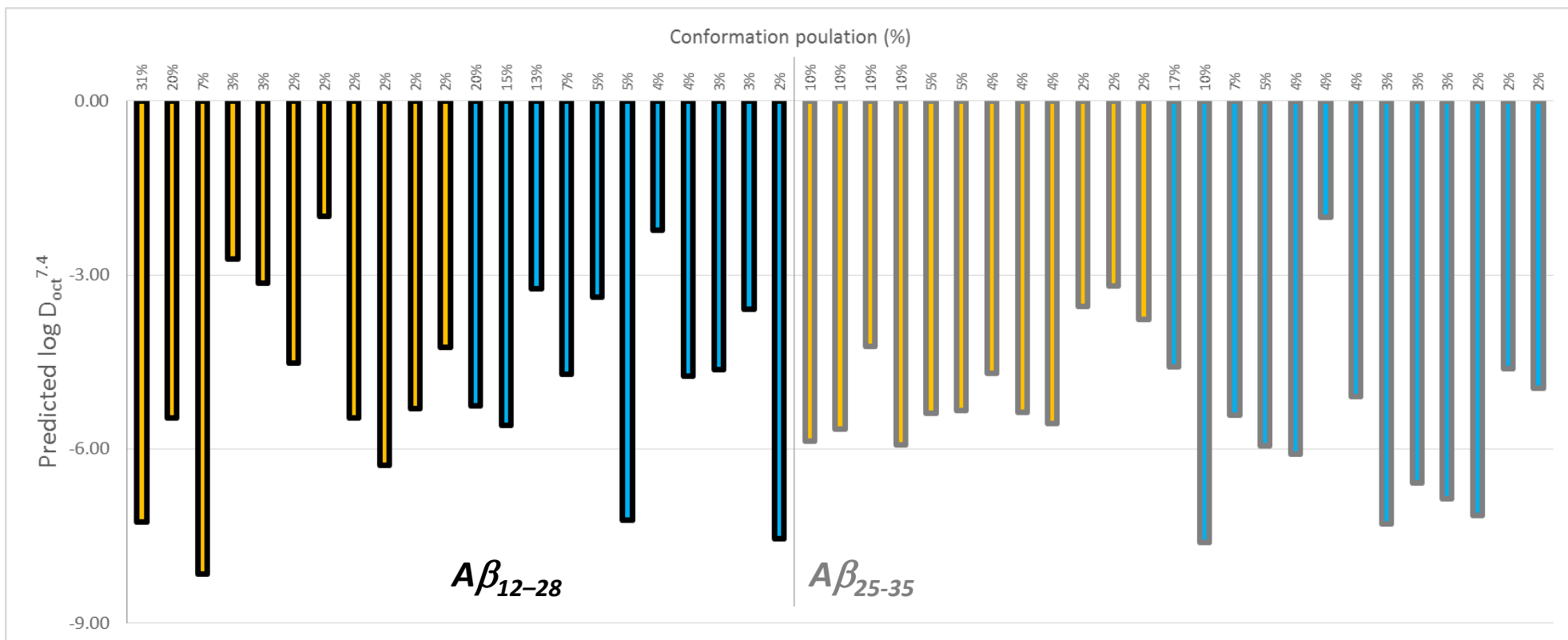


Figure 3

Figure 3

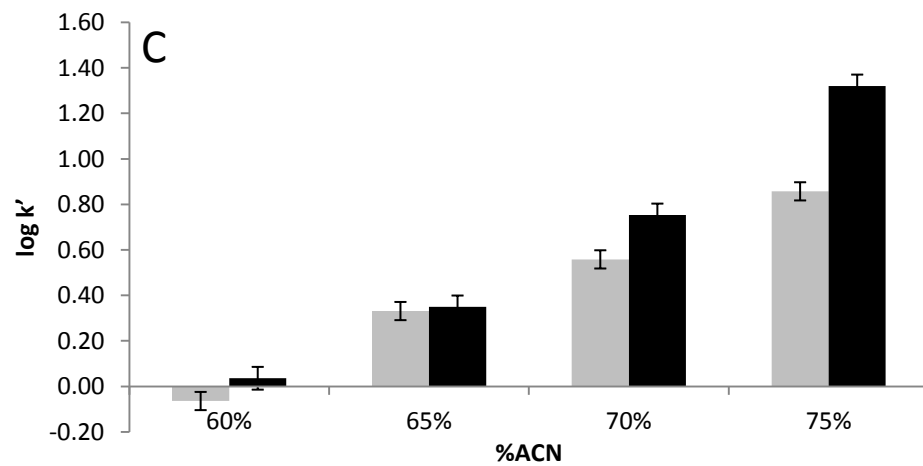
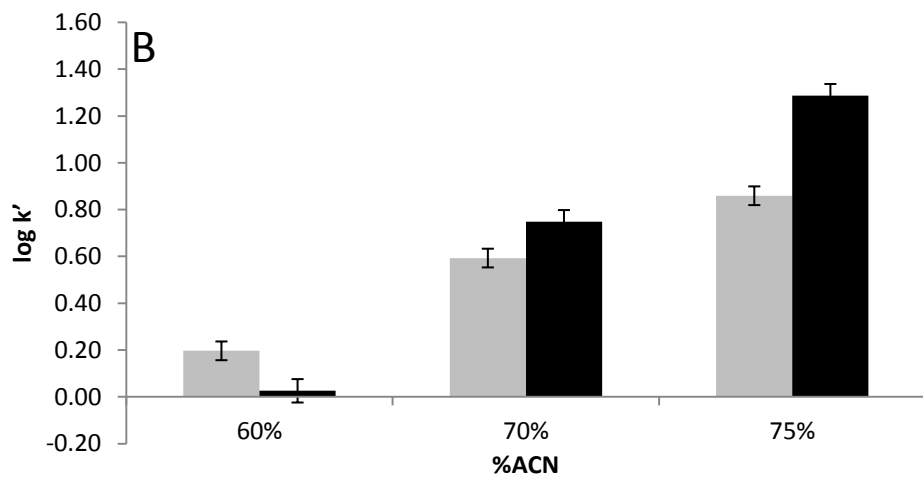
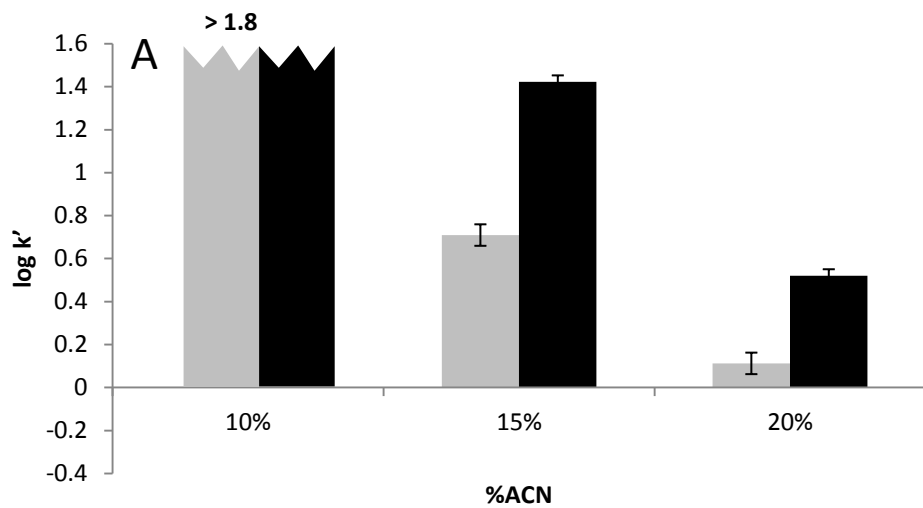


Figure 4

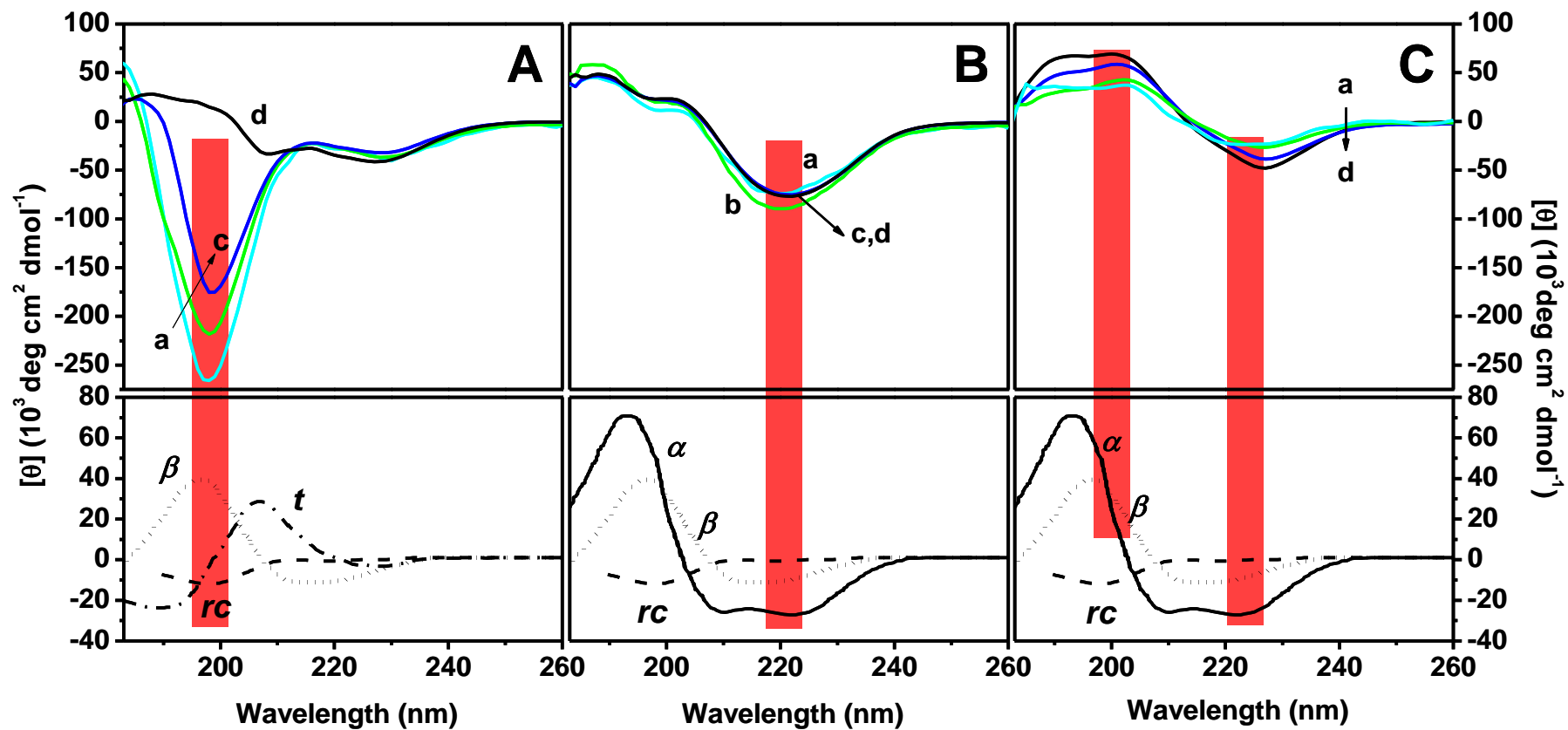
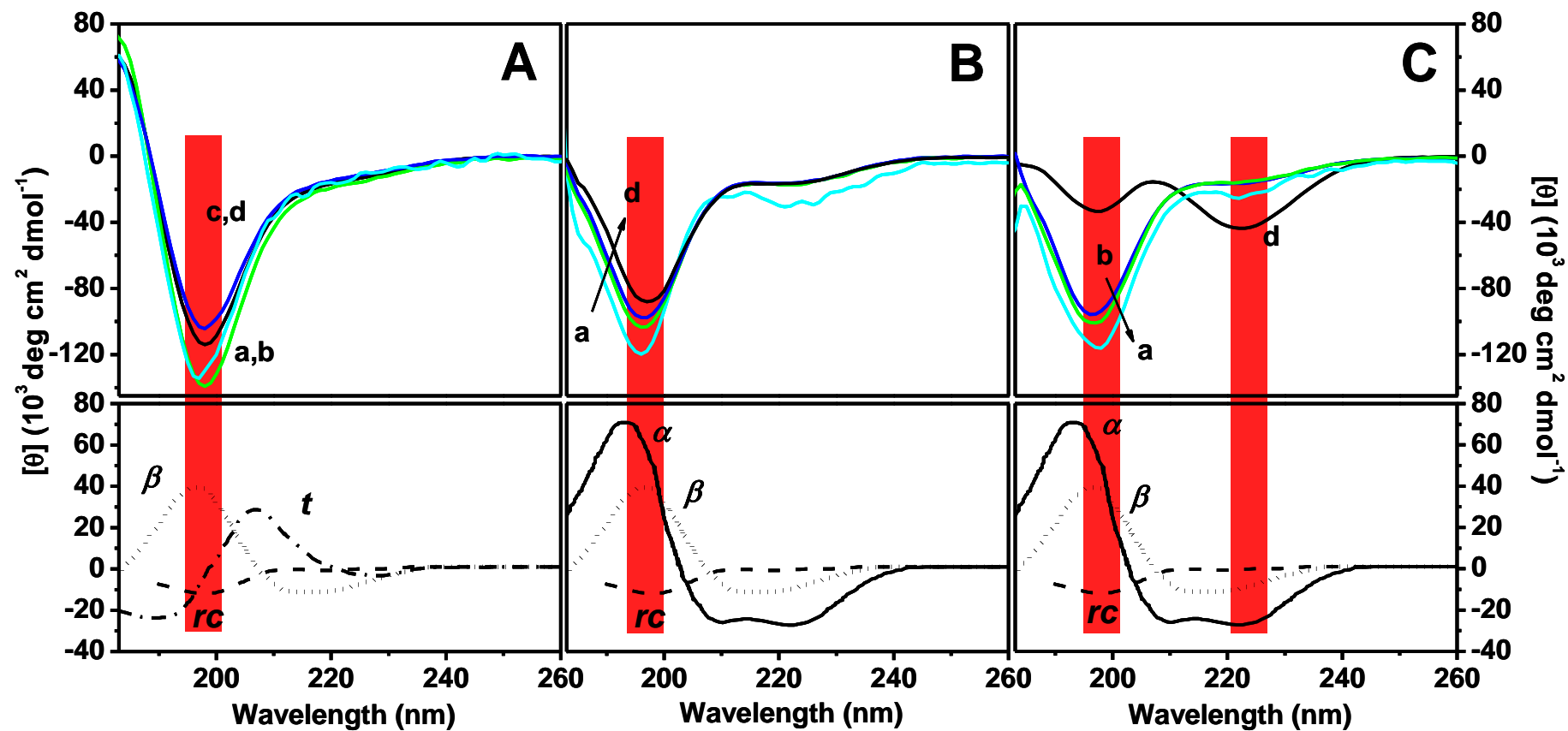


Figure 5



**Supplementary Material**

[Click here to download Supplementary Material: gcaron\\_ijp\\_SupplementaryMaterial.docx](#)